

STEADY-STATE MULTIPLE DARK SPATIAL SOLITONS IN CLOSED-CIRCUIT PHOTOVOLTAIC MEDIA

© 2013 г. Y. H. Zhang*; X. H. Hu**; K. Q. Lu**; B. Y. Liu*; W. Y. Liu*; R. L. Guo*

* Xi'an Technological University, Xi'an, China 710032

** State Key Laboratory of Transient Optics and Photonics, Xi'an Institute of Optics and Precision Mechanics, Chinese Academic of Sciences, Xi'an, China 710119

E-mail: zhangyh1979@163.com

We theoretically study the formation of the steady state multiple dark photovoltaic solitons in the closed-circuit photovoltaic photorefractive crystal. The results indicate that the formation of the multiple dark photovoltaic solitons in the closed-circuit photovoltaic crystal is dependent on the initial width of the dark notch at the entrance face of the crystal. The number of the solitons generated increases with the initial width of the dark notch. If the initial width of the dark notch is small, only a fundamental soliton or Y-junction soliton pair is generated. As the initial width of the dark notch is increased, the dark notch tends to split into an odd (or even) number of multiple dark photovoltaic solitons sequence, which realizes a progressive transition from a lower-order soliton to a higher-order solitons sequence. When the multiple solitons are generated, the separations between adjacent dark solitons become slightly smaller. The soliton pairs far away from the center have bigger width and less visibility and they move away from each other as they propagate in the photorefractive nonlinear crystal.

Keywords: photorefractive spatial solitons, photovoltaic effect, multiple solitons splitting, beam propagation method, close-circuit condition.

Codes OCIS: 190.0190.

Submitted 20.12.2012.

СТАЦИОНАРНЫЕ МНОЖЕСТВЕННЫЕ ТЕМНЫЕ ПРОСТРАНСТВЕННЫЕ СОЛИТОНЫ В ФОТОГАЛЬВАНИЧЕСКИХ СРЕДАХ С ЗАМКНУТЫМ ЭЛЕКТРИЧЕСКИМ КОНТУРОМ

Теоретически изучено формирование стационарных множественных темных фотогальванических солитонов в фотогальваническом кристалле с замкнутым электрическим контуром. Показано, что процесс формирования таких солитонов зависит от начальной ширины провала интенсивности на входной грани кристалла. При увеличении ширины провала число солитонов возрастает. Если начальная ширина провала мала, генерируется только фундаментальный солитон или солитонная пара Y-соединения. При возрастании начальной ширины провала проявляется тенденция к его расщеплению на серию нечетного (или четного) числа множественных темных фотогальванических солитонов, в которой реализуется последовательный переход от солитона низкого порядка к набору солитонов более высокого порядка. Когда генерируются множественные солитоны, расстояния между соседними темными солитонами слегка уменьшается. Солитонные пары вдали от центра обладают большей шириной и меньшим контрастом, и они удаляются друг от друга при распространении в фотогальваническом нелинейном кристалле.

Ключевые слова: фотогальванические пространственные солитоны, фотогальванический эффект, множественное расщепление солитонов, метод распространения излучения, условие замкнутого электрического контура.

1. Introduction

Photorefractive spatial solitons [1–4] are self-trapped non-diffracting light beams or dark notches. They are generated when diffraction

is exactly compensated by the nonlinear self-focusing (or self-defocusing) effect in nonlinear photorefractive media. In the past two decades, photorefractive spatial solitons have become a major field of research in nonlinear optics due

to their potential applications, such as all-optical beam switching and routing, optical interconnects, and reconfigurable soliton-induced waveguides [5–8]. At present, photorefractive spatial solitons are generally classified into four generic types: quasi-steady-state solitons, screening solitons, photovoltaic solitons and screening-photovoltaic solitons. Photovoltaic solitons are distinct from other photorefractive spatial solitons because they do not necessitate application of an external field but only rely on the photovoltaic effect in the photorefractive crystal. Since Valley [9] et al predicted the existence of the photovoltaic spatial solitons in 1994, the investigation on photovoltaic spatial solitons demonstrated much interest. Dark photovoltaic solitons can be formed in self-defocusing photovoltaic-photorefractive media, in which the refractive index of the medium decreases in the illuminated regions while the refractive index in the region of the dark notch remains unchanged. For the dark photovoltaic soliton, a Y-junction soliton and a fundamental soliton were firstly observed experimentally in steady state regime [10, 11]. Theoretically, the characteristics of the fundamental dark photovoltaic soliton in open-circuit and closed-circuit cases were analyzed [12]. However, there is no available theory to explain the formation of a Y-junction soliton. In addition, the quasi-steady state multi-dark-solitons [13, 14] were observed experimentally in $\text{LiNbO}_3:\text{Fe}$ crystal by increasing the illumination time with a fixed incident power. The phenomena occurred in both the amplitude mask and the phase mask. It is a pity that there was not a related theory to plain the phenomena. Up to 2003, M. Chauvet [15] built up a theoretical model to characterize the time-dependent formation of one-dimensional dark photovoltaic solitons under open-circuit conditions. A year later, based on the theoretical model for time-dependent photovoltaic solitons, G. Couton et al used beam propagation method (BPM) to simulate numerically the evolution of the notch-bearing beam inside photovoltaic crystal [16]. The numerical results demonstrated that the multiple solitons occurred in transient (i.e., quasi-steady state) regime. Here, the profile of the dark notch at the entrance of the crystal was described by hyperbolic tangent function. Meanwhile, they observed experimentally the self-formation of one-dimensional multiple dark-grey photovoltaic solitons in the quasi-steady state regime. In addition, Bodnar [17] reported that he also utilized BPM to simu-

late the propagation of the steady state multiple dark photovoltaic solitons by using three given especial functions describing the dark notch in 2007. The simulation results indicated that an odd (or even) number of dark solitons was formed in odd (or even) initial conditions. However, he hasn't observed experimentally the multiple dark solitons sequence. Our research team also simulated numerically the evolution of the multiple dark photovoltaic spatial solitons in steady state and quasi-steady state under open-circuit conditions [18, 19]. We differ from them in that the function describing the dark notch is obtained by solving the solitons equation, rather than special function.

In fact, besides the multiple dark solitons observed on the photovoltaic media, the multiple dark solitons have been theoretically predicted and experimentally observed in Kerr nonlinear media [20–23] and biased photorefractive crystal [24–27] by using coherent light source.

All these investigations on multiple spatial solitons in photovoltaic media were performed in open-circuit conditions. In this paper, we aim to investigate theoretically the formation of steady state multiple dark photovoltaic solitons under closed-circuit conditions by using BPM. The simulation results indicate that a single dark notch with a properly input width can split into multiple dark notches in a closed-circuit self-defocusing nonlinear photovoltaic medium. The initial profile of the dark notch at the entrance of the photovoltaic crystal is obtained by solving the nonlinear Schrödinger equation which describes the propagation of the photorefractive spatial soliton in photorefractive media. Firstly, we solve the nonlinear NSL to obtain a fundamental dark soliton profile by utilizing the fourth order Runge-Kutta algorithm. Then, we utilized the BPM to numerically simulate the evolution of closed-circuit dark photovoltaic solitons. If we expand the width of the dark notch, we find that the dark notch on the otherwise uniform optical beam can split into multiple dark notches, realizing the transformation from a fundamental soliton to an odd-number sequence of multiple dark solitons or from a Y-junction soliton to an even-number sequence of multiple dark solitons. The number of solitons increases with the width of the dark notch. The characteristics of the multiple dark photovoltaic solitons in closed-circuit photovoltaic nonlinear media are similar to that of the multiple dark photovoltaic solitons in open-circuit conditions.

2. Theoretical treatment

To start, let us assume that a coherent beam uniformed along the y direction propagates in a photovoltaic crystal along the z axis and is allowed to diffract only along the x axis. In addition, we assume that the coherent beam is linearly polarized along the x direction. For demonstration purposes, let the photorefractive crystal be LiNbO₃ with its optical c -axis oriented along the x coordinate. Under these conditions, the perturbed refractive index along the x -axis is given by $(n_e')^2 = n_e^2 - n_e^4 r_{33} E_{sc}$, where n_e is the unperturbed extraordinary index of refraction, r_{33} is the electro-optic coefficient of the LiNbO₃ crystal, E_{sc} is the induced space-charge electric field inside the crystal. Therefore, the refractive index variation arising from the space charge field is $\Delta n_e = -1/2 n_e^3 r_{33} E_{sc}$. Under close-circuit condition the steady state equation for the 1D space charge field [12] is given by

$$E = \frac{E_{sc}}{E_p} = \frac{J - I/I_d}{1 + I/I_d}, \quad (1)$$

where E is normalized space charge field, $I = I(x, z)$ is the intensity of the optical beam, E_p is the photovoltaic field constant, I_d is dark irradiance, J is the normalized current density inside the crystal. This expression for the space-charge field is valid for any input beam intensity distribution when the photorefractive effect is governed by the photovoltaic effect in a crystal in close-circuit conditions.

Theoretically, the solution for a one-dimensional dark photovoltaic spatial soliton propagating along the z axis is described by the nonlinear Schrödinger equation

$$\left(\frac{\partial}{\partial z} - \frac{i}{2k} \frac{\partial^2}{\partial x^2} \right) A(x, z) = i \frac{k}{n_e} \Delta n_e A(x, z), \quad (2)$$

where $k = (2\pi/\lambda_0)n_e$ is the wave number in the photorefractive crystal, $A(x, z)$ is the slowly varying amplitude of the input optical field. The dimensionless parameters $\xi = x/d$ and $\zeta = z/(kd^2)$ are the scaled transverse and longitudinal coordinates. Where $d = (\pm(kn_e)^2 r_{33} E_p)^{-1/2}$ is the characteristic length scale. Therefore, propagation Eq. (2) becomes

$$\left(\frac{\partial}{\partial \zeta} - \frac{i}{2} \frac{\partial^2}{\partial \xi^2} \right) \Phi(\xi, \zeta) = \pm \frac{i}{2} \frac{J - r|\Phi|^2}{1 + r|\Phi|^2} \Phi(\xi, \zeta), \quad (3)$$

where $\Phi(\xi, \zeta)$ is the slowly varying amplitude of the optical field in units of $(rI_d)^{1/2}$, r is the ratio of soliton peak intensity I_{\max} to dark irradiance

I_d . For a fundamental dark soliton, the solution can be written as $\Phi(\xi, \zeta) = u(\xi)\exp(i\Gamma kd^2\zeta)$, where $u(\xi)$ is the normalized soliton profile, which depends only on ξ , and Γ is the soliton propagation constant. In this particular case, Eq. (3) becomes

$$u''(\xi) = 2kd^2\Gamma u(\xi) \pm \frac{J - r|u(\xi)|^2}{1 + r|u(\xi)|^2} u(\xi). \quad (4)$$

The sign that is to be retained for the second part of Eq. (4) is identical to the sign of the product $-r_{33}\beta_{ph}$, where β_{ph} is photovoltaic constant. A plus sign is selected for the purpose of generating dark soliton. In our calculation, we numerically integrate Eq. (4) and apply boundary conditions of dark soliton $u(\infty) = 1$ and $u'(\infty) = 0$ to obtain

$$u'^2(0) = -(2kd^2\Gamma + 1) + \frac{J+1}{r} \ln(1+r). \quad (5)$$

In addition, by applying boundary conditions of dark solitons $u(\infty) = 1$ and $u''(\infty) = 0$ in Eq. (4), the soliton propagation constant can be obtained

$$\Gamma = \frac{J - r}{2kd^2(1+r)}. \quad (6)$$

In order to yield the spatial profile of the fundamental dark soliton, Eq. (4) is integrated numerically by the fourth order Runge–Kutta algorithm combined with initial conditions of dark soliton $u'(0)$ and $u(0) = 0$. Here, for short-circuit case $J \rightarrow lru_\infty^2/[\Delta x(1 + ru_\infty^2) + l]$ [12, 28] and for open circuit case $J = 0$. When $l \gg \Delta x$ case and $r \ll 1000$, we obtain $J \approx ru_\infty^2$ for short-circuit case. The step size used is 10^{-3} . The calculated relative error and absolute error in the simulation process are 10^{-6} .

3. Numerical simulations results

In our numerical simulations, we choose LiNbO₃ as photovoltaic-photorefractive crystal, the crystal-dependent parameters of whose are $n_e = 2.2$, $r_{33} = 30$ pm/V, $E_p = 7.7 \times 10^6$ V/m, $\lambda_0 = 0.5$ μ m, the transverse distance of the crystal $l = 4$ mm.

Under above conditions, we obtain the existence curves of the fundamental dark soliton in open-circuit and short-circuit conditions showed in Fig. 1. The existence curves give the relationship among the width, amplitude, nonlinearity, and optical wavelength in the medium and indicate that the full width at half-maximum (FWHM) of the fundamental dark soliton is a function of the ratio r of soliton peak inten-

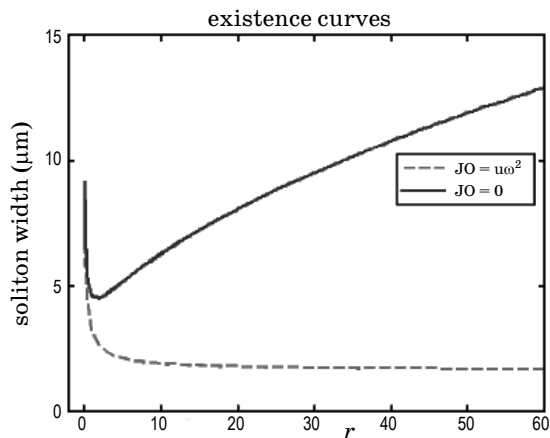


Fig. 1. Existence curves for steady state fundamental dark photovoltaic spatial soliton in open-circuit (solid curve) and short-circuit (dashed curve) cases.

sity to dark irradiance for the given nonlinearity, and optical wavelength. From the curves, we note that the intensity FWHM of the fundamental dark soliton both in open-circuit and closed-circuit cases acutely and monotonously decreases with r when the r is small. The width of them is equal. When the r is bigger, the width of the closed-circuit dark soliton monotonously and slowly decreases, however the width of open-circuit dark soliton acutely and monotonously increases. This implies that a lower nonlinearity is needed to self-trap a closed-circuit dark soliton with the same initial input width in the same medium.

In the following numerical simulations, we achieve the transform from a fundamental soliton or a Y-junction soliton to the multiple dark solitons by expanding the input width of the dark notch Δx . Firstly, we calculate $\Phi(\xi, 0)$ by solving Eq. (4) numerically with the fourth order Runge–Kutta algorithm and then expand the intensity FWHM of the fundamental dark soliton. Then, Eq. (3) is solved numerically by BPM to obtain the evolution of the multiple solitons. In our calculations, we divide the propagation distance into many steps in which the step size dz is designated as $1 \mu\text{m}$, i.e. $d\zeta = 0.03$. At every step, the diffraction effect is first considered exclusively, and then only the nonlinear term is calculated.

3.1. Short-circuit case

(a) Low input optical intensity

In the following simulations, we assume $r = 1$. Under this condition, $J_{\text{max}} = 1$ is corresponding

to short-circuit case, thus the values of J can range from $[0]$ to 1 .

For a closed-circuit odd-phased input beam, a soliton solution of Eq. (4) can be found and it describes a $3 \mu\text{m}$ fundamental dark soliton for $J = r$ when $r = 1$. For illustration the evolution of the beam profiles is plotted in Fig. 2 with a maximum propagation distance of 1 cm . Fig. 2(a) shows the propagation of such a fundamental dark soliton. A constant beam profile is obtained throughout the crystal. When the width of the initial input dark notch is increased, the odd-phased beam tends to split into an odd-number sequence of multiple dark solitons. For instance, Fig. 2(b) shows the triple-solitons structure consisting of two side lobes and a central lobe, in which the FWHM value of the input beam profile is $8 \mu\text{m}$. The two side lobes are less visible. If the intensity FWHM of the input beam is further increased, a secondary set of lobes with less visibility symmetrically starts to appear on the two sides. Fig. 2(c) and (d) show the $N = 5$ and $N = 7$ splitting process of the initial dark notches for $\Delta x_5 = 15 \mu\text{m}$ and $\Delta x_7 = 19 \mu\text{m}$ respectively. If we increase further FWHM of the beam's intensity, we can observe more and more pairs of side lobes developing with less visibility, forming the higher-order odd-number sequence dark photovoltaic spatial solitons.

For a closed-circuit even-phased input beam, the dark notch always tends to split into two dark solitons when the intensity FWHM of the initial input beam is small. Fig. 3(a) shows the Y splitting of the dark notch with $\Delta x_2 = 6 \mu\text{m}$. The width of each lobe and the deep of the intensity are equal. When the width of the dark notch increases, in a manner similar to that of an odd-phased beam, more and more soliton pairs appear symmetrically on either side of the Y-junction soliton splitting, which indicates the formation of high-order solitons. Fig. 3(b) and (c) show the $N = 4$ and $N = 6$ soliton splitting process for $\Delta x_4 = 10 \mu\text{m}$ and $\Delta x_6 = 16 \mu\text{m}$ respectively. Fig. 3(d) shows the $N = 8$ solitons splitting process for $\Delta x_8 = 26 \mu\text{m}$. If we increase the width of the dark notch, the more solitons pair with less visibility will appear in two sides, forming higher-order multiple solitons.

(b) High input optical intensity

When the input optical intensity is bigger, the input width required to form the multiple dark photovoltaic solitons is small relative to that of open-circuit conditions [18, 19]. When the input width of the dark notch is bigger, the optical in-

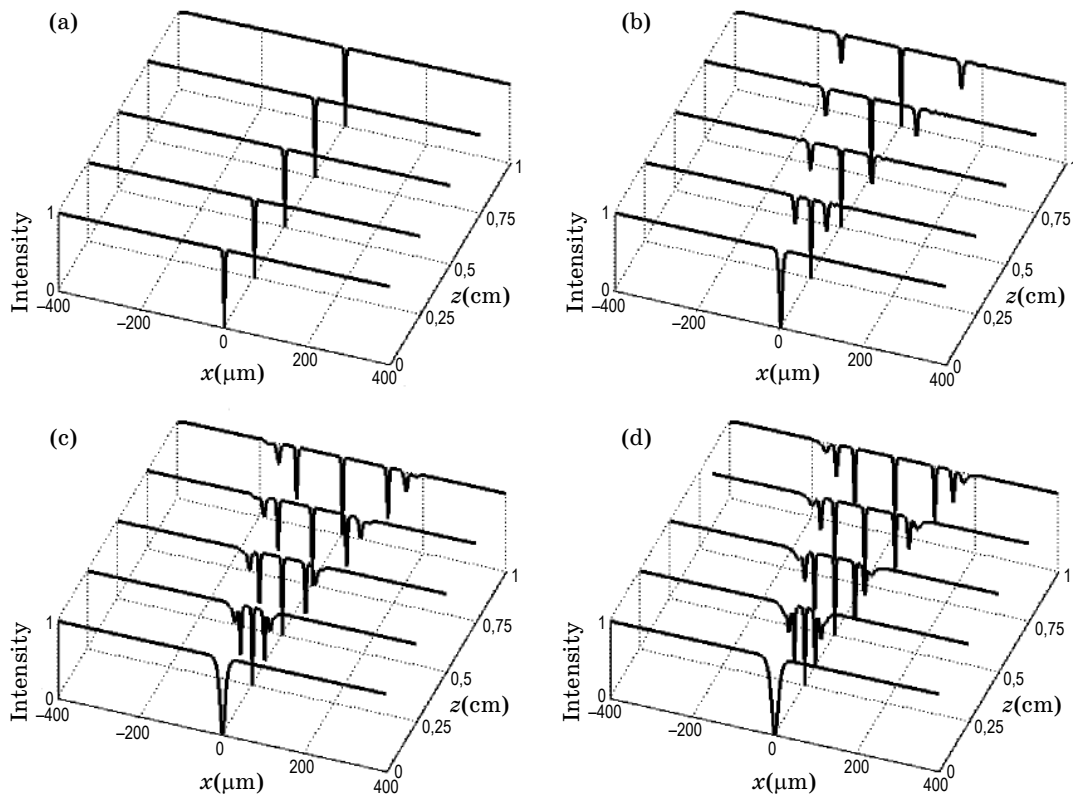


Fig. 2. Formation of the odd number of multiple dark photovoltaic solitons sequence in the short-circuit case. (a) Propagation of a 3 μm , fundamental dark soliton. (b) An 8 μm wide dark notch splits into three dark solitons stripes. (c) A 15 μm wide dark notch splits into five dark solitons stripes. (d) A 19 μm wide dark notch splits into seven dark solitons stripes. In all case $r = 1$, $z = 1$ cm.

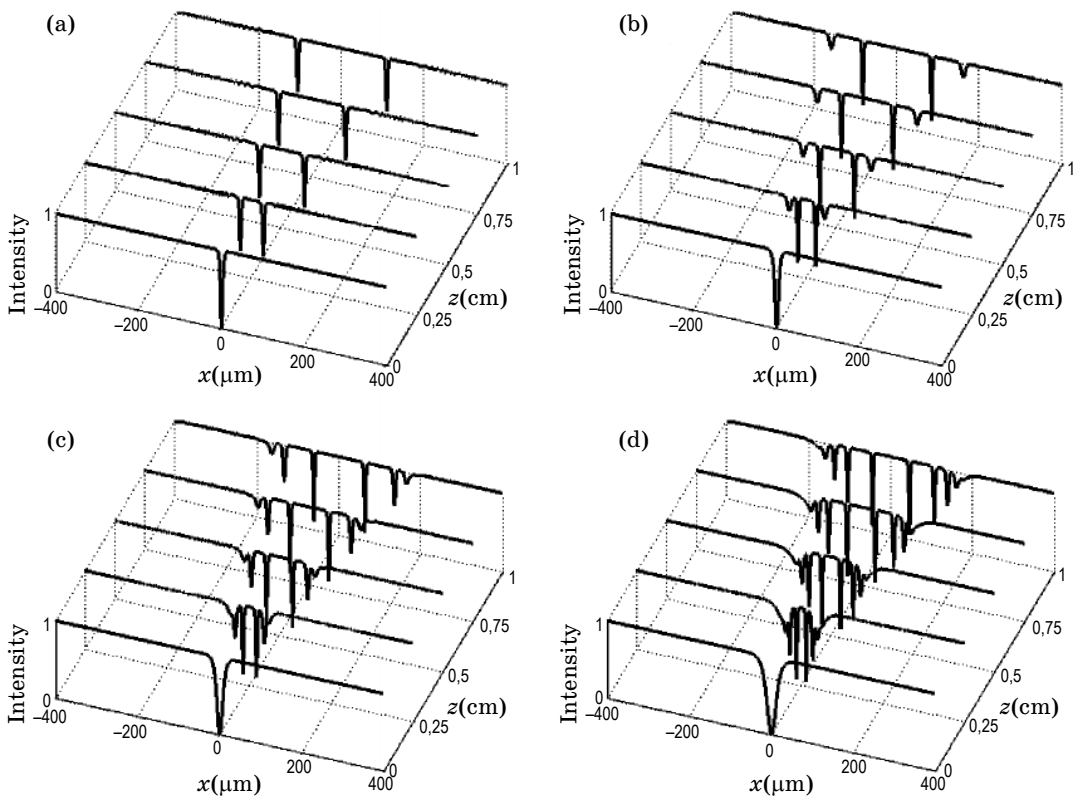


Fig. 3. Formation of the even number of multiple dark photovoltaic solitons in short-circuits case. (a) Propagation of a 6 μm dark notch splits into Y-junction soliton pair. (b) A 10 μm wide, dark notch splits into four dark solitons. (c) A 16 μm wide, dark notch splits into six dark solitons. (d) A 26 μm wide dark notch splits into eight dark solitons. In all case $r = 1$, $z = 1$ cm.

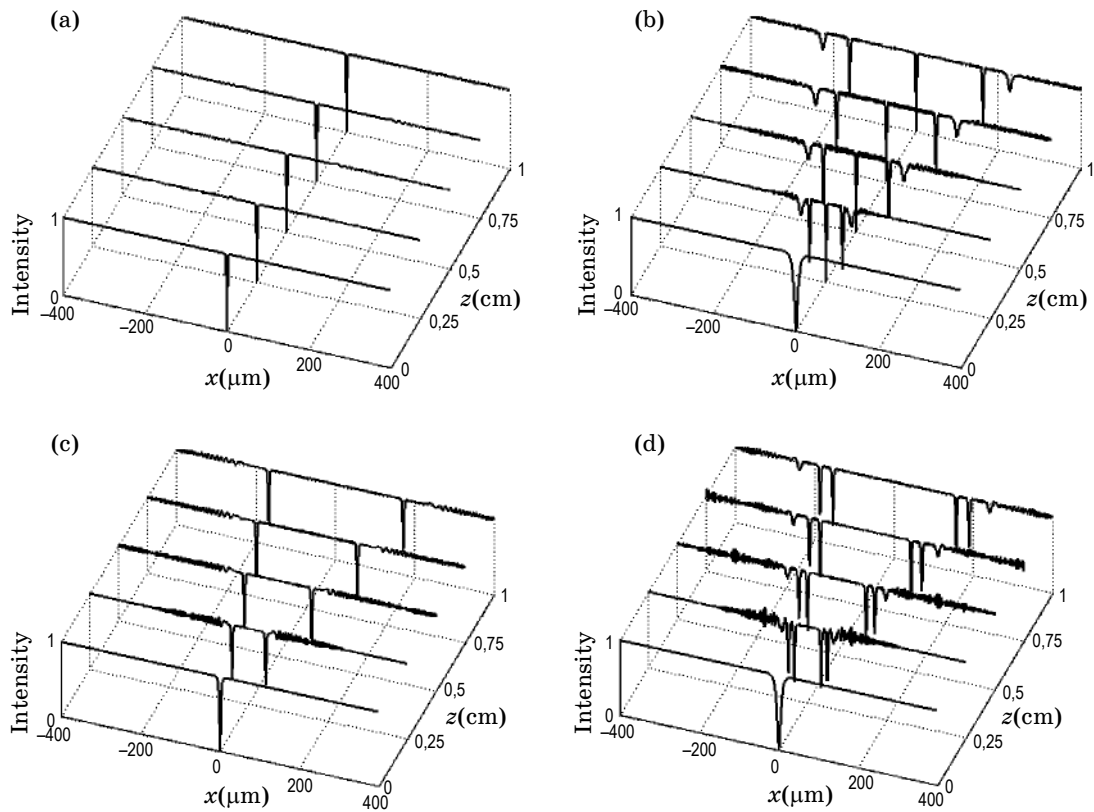


Fig. 4. Formation of the even number of multiple dark photovoltaic solitons in short-circuits case. (a) Propagation of a $1.7 \mu\text{m}$ fundamental dark soliton. (b) A $10 \mu\text{m}$ wide, dark notch splits into five dark solitons. (c) A $4 \mu\text{m}$ wide, dark notch splits into Y-junction dark solitons. (d) A $10 \mu\text{m}$ wide dark notch splits into six dark solitons. In all case $r = 30$, $z = 1 \text{ cm}$.

tensity around the multiple solitons has small vibration. In addition, the separations between soliton pair in the center barely change relative to the Y-junction soliton while the even-number sequence of the multiple dark solitons is generated. The results are showed in Fig. 4.

3.2. Open-circuit case

For an open-circuit odd-phase beam, a soliton solution of Eq. (4) is found and it describes a $4.6 \mu\text{m}$ fundamental dark soliton for $r = 1$. Fig. 5(a) shows the propagation of such a fundamental dark soliton in open-circuit photovoltaic crystal. The beam profile is obtained throughout the crystal. When the FWHM of the beam's intensity is increased, the odd-phased beam tends to split into an odd-number sequence of multiple dark solitons, which is similar to the multiple dark solitons splitting in closed-circuit condition. For instance, Fig. 5(b) shows the triple-solitons structure consisting of two side lobes and a central lobe, which FWHM is $10 \mu\text{m}$. The

minimum intensity of the two side lobes is less visible. If we further increased the width of the initial input dark notch, a secondary set of lobes with less visibility symmetrically starts to appear on the two sides. Fig. 5(c) shows the $N = 5$ splitting found for $\Delta x_5 = 18 \mu\text{m}$. If we increase further FWHM of beam's intensity, we can observe more and more pairs of side lobes developing with less visibility, forming the higher-order odd number sequence of dark photovoltaic spatial solitons.

For an open-circuit even-phased input beam, the dark notch always tends to split into two notches when the FWHM is small. Fig. 6(a) shows the Y splitting found for $\Delta x_2 = 8 \mu\text{m}$. The width of each lobe and the deep of the intensity are equal. As the FWHM is further increased, in a manner similar to that of an odd-phased beam, more secondary sets of lobes appear symmetrically on either side of the Y-junction soliton splitting. Fig. 6(b) and (c) show the $N = 4$ and $N = 6$ soliton splitting for $\Delta x_4 = 17 \mu\text{m}$ and $\Delta x_6 = 26 \mu\text{m}$ respectively. If we increase the

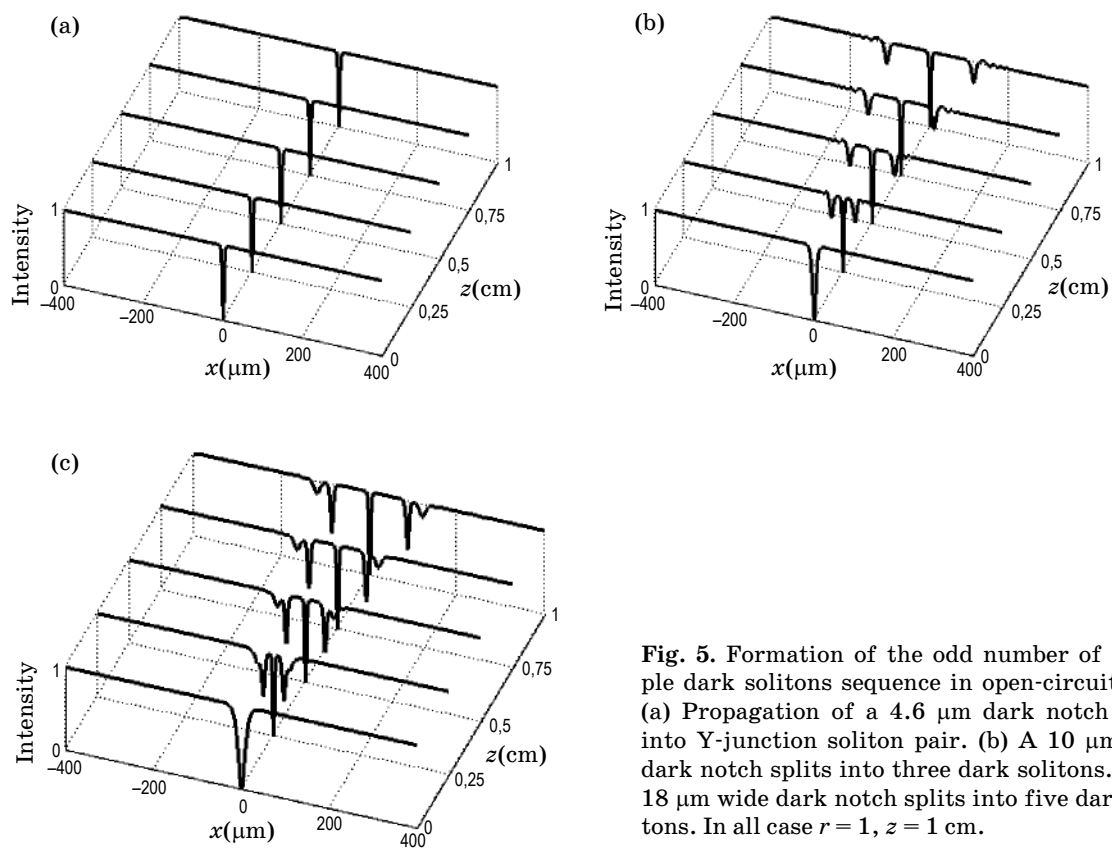


Fig. 5. Formation of the odd number of multiple dark solitons sequence in open-circuit case. (a) Propagation of a 4.6 μm dark notch splits into Y-junction soliton pair. (b) A 10 μm wide dark notch splits into three dark solitons. (c) An 18 μm wide dark notch splits into five dark solitons. In all case $r = 1$, $z = 1$ cm.

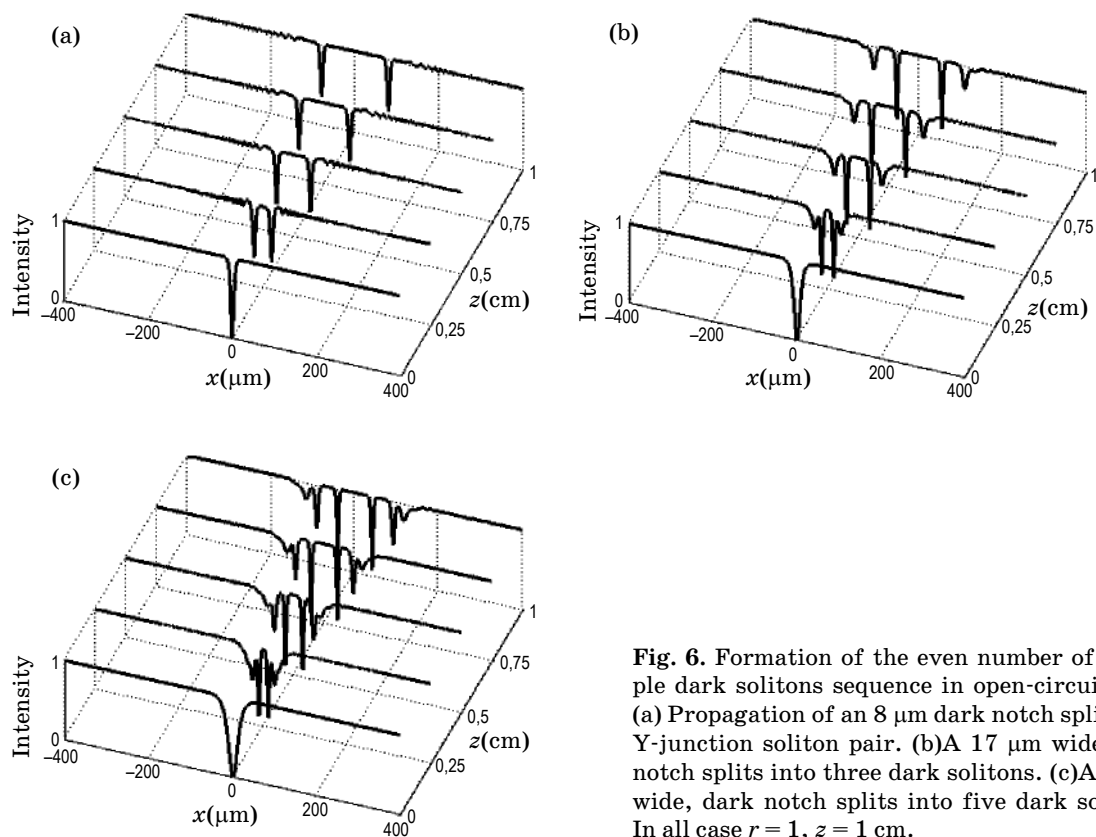


Fig. 6. Formation of the even number of multiple dark solitons sequence in open-circuit case. (a) Propagation of an 8 μm dark notch splits into Y-junction soliton pair. (b) A 17 μm wide, dark notch splits into three dark solitons. (c) A 26 μm wide, dark notch splits into five dark solitons. In all case $r = 1$, $z = 1$ cm.

width of the dark notch, the more solitons pair with less visibility will appear in two sides, forming higher order multiple solitons.

From Fig. 2 to 6, we note that formation of the multiple dark solitons in closed-circuit conditions is similar to open-circuit multiple dark photovoltaic solitons. However, for a given input optical beam's intensity, forming the multiple solitons with the same number in the closed-circuit conditions needs smaller width than open-circuit solitons. For example, when the width of the dark notch is 26 μm , the dark notch splits into eight dark notches in short-circuit case showed in Fig. 3(d), however, it can split into six dark notches in open-circuit case showed in Fig. 6(c).

4. Conclusions

In summary, we have shown that the multiple dark spatial solitons sequence for closed-circuit case can be formed in photovoltaic-photorefractive crystal when they evolve from a single dark notch. We have simulated numerically the evolution of the steady state multiple dark photovoltaic spatial solitons sequence by using BPM. The results indicate that the generation of multiple dark photovoltaic spatial solitons under short-circuit case is dependent on the initial input conditions, current density J and the ini-

tial input width of the dark notch and that the formation of the closed-circuit multiple dark solitons requires lower nonlinearity than the open-circuit multiple dark solitons. The number of solitons generated increases notably with the width of the dark notch with given r and J . When the width of the dark notch is small, it tends to split into a fundamental dark soliton or Y-junction gray soliton. When the width of the dark notch is increased, an odd (or even) number sequence of multiple dark photovoltaic solitons can be formed under appropriate initial conditions. They move away from each other as they propagate in the photorefractive nonlinear crystal. Furthermore, solitons pairs become progressively wider and less visible as their transverse distance from the central dark soliton increases. Previous studies on steady state photorefractive screening solitons [24–27] and quasi-steady state photovoltaic solitons [16] revealed the similar property. The waveguide that is induced by the multiple dark solitons during the formation of solitons could be used to create reconfigurable optical circuits such as beam couplers or multiplexers. The number of outputs could be modified by adjusting the initial input width of the dark notch.

This work has been supported by the National Natural Science Foundation of China under Grant no.10674176.

* * * * *

REFERENCES

1. *DelRe E, Crosignani B., Porto P.D.* Photorefractive spatial solitons. Springer Series in Optical Sciences. 2001. 82. Spatial Solitons. Chap IV. P. 61–86.
2. *DelRe E., Segev M.* Self-focusing and solitons in photorefractive media. Topics in Appl. Phys. 2009. V. 114. P. 547–572.
3. *Królikowski W., Davies B.L., Denz C.* Photorefractive Solitons. IEEE J. Quant. Electron. 2003. V. 39. P. 3–12.
4. *Weilnau C., Ahles M., Petter J., et al.* Spatial optical (2+1)-dimensional scalar- and vector-solitons in saturable nonlinear media. Ann. Phys. 2002. V. 11. P. 573–629.
5. *Kip D., Herden C., Wesner M.* All-optical signal routing using interaction of mutually incoherent spatial solitons. Ferroelectrics. 2002. V. 274. P. 135–142.
6. *Guo A., Henry M., Salamo G.J., et al.* Fixing multiple waveguides induced by photorefractive solitons: directional couplers and beam splitters. Opt. Lett. 2001. V. 26. № 16. P. 1274–1276.
7. *Asaro M., Sheldon M., Chen Z.G., et al.* Soliton-induced waveguides in organic photo-refractive glass. Opt. Lett. 2005. V. 30. № 5. P. 519–521.
8. *Lu Y., Liu S.M., Zhang G.Q., et al.* Waveguides and directional coupler induced by white-light photovoltaic dark spatial solitons. J. Opt. Soc. Am. B. 2004. V. 21. № 9. P. 1674–1678.

9. Valley G.C., Segev M., Crosignani B., et al. Dark and bright photovoltaic spatial solitons. Phys. Rev. A. 1994. V. 50. № 6. P. R4457–R4460.
10. Taya M., Bashaw M.C., Fejer M.M., et al. Observation of dark photovoltaic spatial solitons. Phys. Rev. A. 1995. V. 52. № 4. P. 3095–3100.
11. Taya M., Bashaw M.C., Fejer M.M., et al. Y-junctions arising from dark-soliton propagation in photovoltaic media. Opt. Lett. 1996. V. 21. № 13. P. 943–945.
12. Segev M., Valley G.C., Bashaw M.C., et al. Photovoltaic spatial solitons. J. Opt. Soc. Am. B. 1997. V. 14. № 7. P. 1772–1778.
13. Zhang G.Q., Liu S.M., Xu J.J., et al. Photorefractive spatial dark-soliton stripes in LiNbO₃: Fe crystal and their application. Chin. Phys. Lett. 1996. V. 13. № 2. P. 101–104.
14. Liu S.M., Zhang G.Q., Tian G.Y., et al. (1+1)-Dimensional and (2+1)-dimensional waveguides induced by self-focused dark notches and crosses in LiNbO₃:Fe crystal. Appl. Opt. 1997. V. 36. P. 8982–8986.
15. Chauvet M. Temporal analysis of open-circuit dark photovoltaic spatial solitons. J. Opt. Soc. Am. B. 2003. V. 20. № 12. P. 2515–2522.
16. Couton G., Maillotte H., Chauvet M. Self-formation of multiple spatial photovoltaic solitons. J. Opt. B: Quantum Semiclass. Opt. 2004. № 6. P. S223–S230.
17. Bodnar M. Dark Photovoltaic Spatial Solitons: Experiment and Numerical Solution. Proc. of SPIE. 2007. V. 6582. 65821 P.
18. Zhang Y.H., Lu K.Q., Guo J.B., Li K.H., Liu B.Y. Steady-state multiple dark photovoltaic spatial solitons. European Physical Journal D. 2012. V. 66. № 3. P. 65–69.
19. Zhang Y.H., Lu K.Q., Guo J.B., Long X.W., Hu X.H., Li K.H. Formation of multiple dark photovoltaic spatial solitons. Pramana-Journal of physics. 2012. V. 78. № 2. P. 265–275.
20. Zakharov V.E., Shabat A.B. Interaction between solitons in a stable medium. Sov. Phys. JETP. 1973. V. 37. № 5. P. 823–825.
21. Blow K.J., Doran N.J. Multiple dark soliton solutions of the nonlinear Schrödinger equation. Phys. Lett. A. 1985. V. 107. P. 55–58.
22. Skinner S.R., Allan G.R., Andersen D.R., Smirl A.L. Dark Spatial Soliton Propagation in Bulk ZnSe. IEEE J. Quant. Electron. 1991. V. 27. № 9. P. 2211–2219.
23. Barry L.D., Yang X.P. Waveguides and Y junctions formed in bulk media by using dark spatial solitons. Opt. Lett. 1992. V. 17. № 7. P. 496–498.
24. Chen Z.G., Mitchell M., Segev M. Steady-state photorefractive soliton-induced Y-junction waveguides and high-order dark spatial solitons. Opt. Lett. 1996. V. 21. № 10. P. 716–718.
25. Chen Z.G., Segev M., Singh S.R., et al. Sequential formation of multiple dark photorefractive spatial solitons: experiments and theory. J. Opt. Soc. Am. B. 1997. V. 14. № 6. P. 1407–1417.
26. Chen Z.G., Segev M. Sequences of high-order dark photorefractive spatial solitons and soliton-induced waveguides formed in bulk SBN. Proc. of SPIE. 1996. V. 2896. P. 148–157.
27. Méndez-Otero M.M., Iturbe-Castillo M.D., Rodríguez-Montero P., et al. High order dark spatial solitons in photorefractive Bi₁₂TiO₂₀ crystal. Opt. Commun. 2001. V. 193. P. 277–282.
28. Lu K.Q., Zhao W., Zhang L., et al. Temporal behavior of dark spatial solitons in closed-circuit photovoltaic media. Opt. Commun. 2008. V. 281. P. 2913–2917.